The Plant Cell, Vol. 24: 3320–3332, August 2012, www.plantcell.org

Gibberellin Regulates the *Arabidopsis* Floral Transition through miR156-Targeted SQUAMOSA PROMOTER BINDING–LIKE Transcription Factors[W]

Sha Yu,[a,b,1] Vinicius C. Galvão,[c,1] Yan-Chun Zhang,[a] Daniel Horrer,[c,2] Tian-Qi Zhang,[a,b] Yan-Hong Hao,[d] Yu-Qi Feng,[d] Shui Wang,[a] Markus Schmid,[c] and Jia-Wei Wang[a,3]

[a] National Key Laboratory of Plant Genetics, Institute of Plant Physiology and Ecology, Shanghai Institutes for Biological Sciences, Shanghai 200032, China

[b] Graduate School of Chinese Academy of Sciences, Beijing 100049, China

[c] Department of Molecular Biology, Max Planck Institute for Developmental Biology, Tuebingen D-72076, Germany

[d] Key Laboratory of Analytical Chemistry for Biology and Medicine (Ministry of Education), Department of Chemistry, Wuhan University, Wuhan 430072, China

Gibberellin (GA), a diterpene hormone, plays diverse roles in plant growth and development, including seed germination, stem elongation, and flowering time. Although it is known that GA accelerates flowering through degradation of transcription repressors, DELLAs, the underlying mechanism is poorly understood. We show here that DELLA directly binds to microRNA156 (miR156)-targeted SQUAMOSA PROMOTER BINDING–LIKE (SPL) transcription factors, which promote flowering by activating miR172 and MADS box genes. The interaction between DELLA and SPL interferes with SPL transcriptional activity and consequently delays floral transition through inactivating miR172 in leaves and MADS box genes at shoot apex under long-day conditions or through repressing MADS box genes at the shoot apex under short-day conditions. Our results elucidate the molecular mechanism by which GA controls flowering and provide the missing link between DELLA and MADS box genes.

INTRODUCTION

The shoot apical meristem (SAM) of plants continuously produces lateral organs. Based on the identity and morphological traits of the lateral organs, the life cycle of a plant can be divided into two major phases: vegetative and reproductive. The SAM produces leaves during the vegetative phase, whereas it gives rise to flowers in the reproductive phase (Poethig, 2003). The switch from vegetative to reproductive growth, also known as the floral transition, is controlled by both endogenous and exogenous cues, such as age, temperature, photoperiod, and hormones. Molecular and genetic analyses have revealed that the multiple floral inductive cues are integrated via a set of floral-promoting MADS box genes, including *APETALA1* (*AP1*), *SUPPRESSOR OF OVEREXPRESSION OF CO1* (*SOC1*), *FRUITFULL* (*FUL*), and plant-specific transcription factor *LEAFY* (*LFY*) (Amasino, 2010; Lee and Lee, 2010; Srikanth and Schmid, 2011).

In *Arabidopsis thaliana*, the onset of flowering is accelerated by long-day conditions and delayed by short-day conditions. Seasonal changes in daylength are perceived in leaves and transduced to CONSTANS (CO), which activates the expression of *FLOWERING LOCUS T* (*FT*) in the vascular tissues of the leaves (Samach et al., 2000; An et al., 2004; Kobayashi and Weigel, 2007). The FT protein, as the output of the photoperiodic cue, moves from the leaves to the shoot apex, where it binds to the 14-3-3 protein and the transcription factor FD to activate the expression of MADS box genes (Abe et al., 2005; Wigge et al., 2005; Corbesier et al., 2007; Jaeger and Wigge, 2007; Lin et al., 2007; Mathieu et al., 2007; Taoka et al., 2011). In addition to being activated by CO, the expression of *FT* is negatively regulated by other transcriptional regulators, such as *FLOWERING LOCUS C* (*FLC*), *SHORT VEGETATIVE PHASE* (*SVP*), and *TEMPRANILLO* (*TEM*) (Searle et al., 2006; Castillejo and Pelaz, 2008; Li et al., 2008).

Under noninductive short-day conditions, two pathways play critical roles in flowering: one is dependent on the biosynthesis of the plant hormone gibberellin (GA) (Mutasa-Göttgens and Hedden, 2009); another is mediated by microRNA156 (miR156), which targets a group of transcription factors called SQUAMOSA PROMOTER BINDING–LIKEs (SPLs) (Cardon et al., 1999; Rhoades et al., 2002).

The miR156–SPL interaction constitutes an evolutionarily conserved, endogenous cue for both vegetative phase transition and flowering (Huijser and Schmid, 2011). The age-dependent decrease in miR156 results in an increase in SPLs that promote juvenile to adult phase transition and flowering through activation of miR172, MADS box genes, and *LFY* (Wang et al., 2009; Wu et al., 2009; Yamaguchi et al., 2009). Interestingly, SPLs not

[1] These authors contributed equally to this work.

[2] Current address: Institute of Plant Biology, University of Zürich, CH-8008 Zurich, Switzerland.

[3] Address correspondence to jwwang@sibs.ac.cn.

The author responsible for distribution of materials integral to the findings presented in this article in accordance with the policy described in the Instructions for Authors (www.plantcell.org) is: Jia-Wei Wang (jwwang@sibs.ac.cn).

[W] Online version contains Web-only data.

www.plantcell.org/cgi/doi/10.1105/tpc.112.101014

only act as the upstream activators of the floral-promoting MADS box genes but also serve as their downstream targets. The expression of three miR156-targeted *SPLs*, namely *SPL3*, *SPL4*, and *SPL5*, is highly induced by photoperiod (Schmid et al., 2003). More recently, *SPL3* has been shown to be directly regulated by SOC1 (Jung et al., 2012), and the transcript level of *SPL4* is reduced in the SAM of the *soc1 ful* double mutant (Torti et al., 2012). This interlocking feed-forward loop might contribute to a rapid and irreversible transition from vegetative to reproductive development.

GA is essential for floral induction in short-day conditions, because the plants that harbor the mutation in a GA biosynthetic gene, such as *GA1*, fail to flower (Wilson et al., 1992). In long-day conditions, the effect of GA on flowering is less pronounced. However, the analyses of the GA receptor mutants indicate that GA also plays an important role in flowering in long-day conditions (Griffiths et al., 2006). Recent studies have demonstrated that the GA response is mediated by the ubiquitin-proteasome pathway (Harberd, 2003; Schwechheimer and Willige, 2009). By binding to a nuclear receptor, GIBBERELLIN INSENSITIVE DWARF1 (GID1), GAs regulate gene expression by promoting the degradation of the transcriptional regulator DELLA proteins, including REPRESSOR OF GA1-3 1 (RGA), GA INSENSITIVE (GAI), RGA-LIKE1 (RGL1), and RGL2 (Murase et al., 2008). The degradation of DELLA proteins is mediated by 17 amino acids, called the DELLA motif (Dill et al., 2001). The *Arabidopsis gai*-1 mutant, which carries a deletion of the DELLA motif, is insensitive to GA-induced proteolysis and delays flowering (Peng

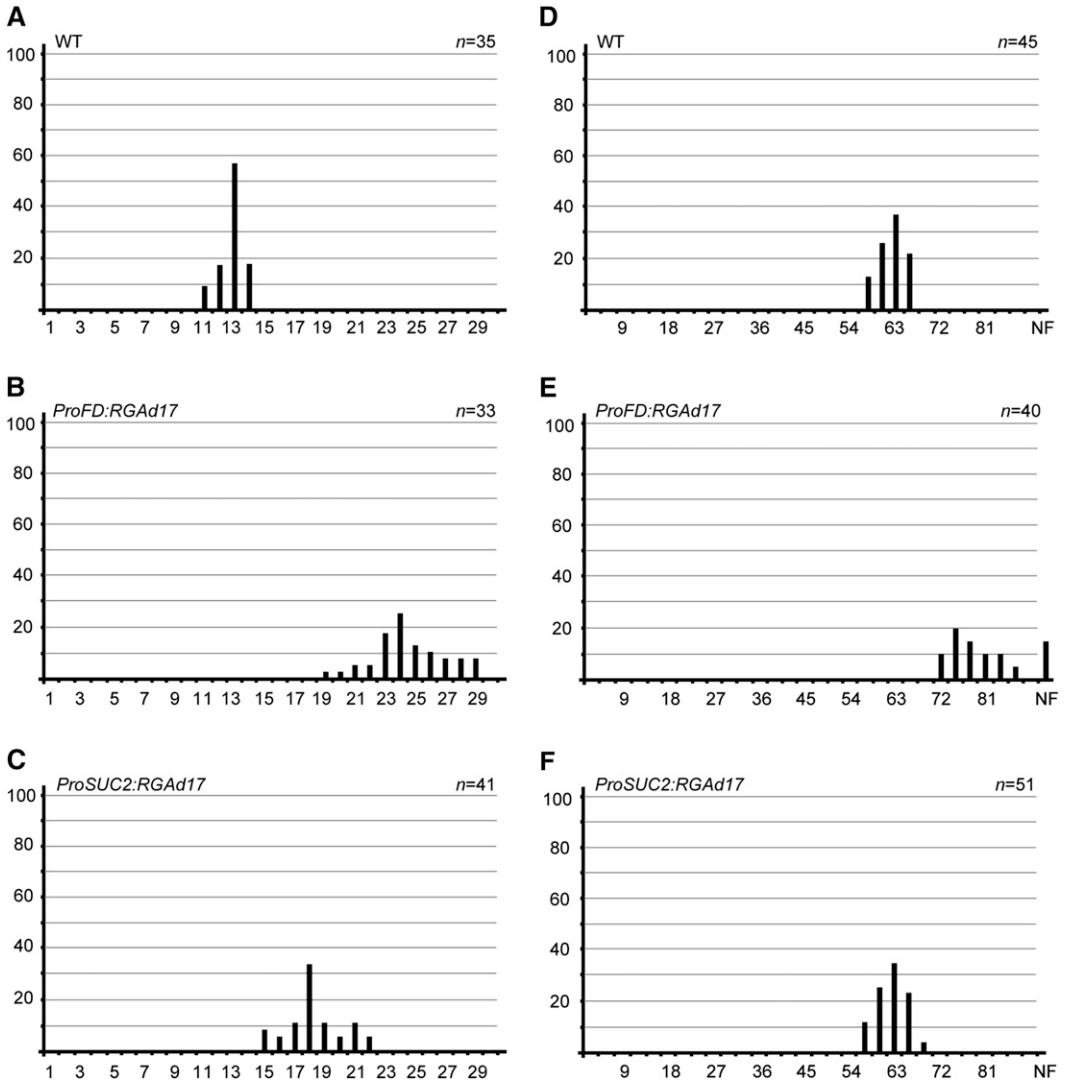

Figure 1. RGA Represses Flowering Both in Leaves and at Shoot Apices.

Flowering time of wild-type (WT), *ProSUC2:RGAd17*, and *ProFD:RGAd17* plants under long-day (**[A]** to **[C]**) or short-day conditions (**[D]** to **[F]**). Flowering frequency of T1 transgenic lines is shown as a histogram, with the *y* axis indicating percentage of plants that flower with a given number of leaves. The *x* axis indicates the number of leaves. NF, never flowering.

et al., 1997; Dill et al., 2001). Although it is known that GA promotes flowering through activating MADS box genes and *LFY* (Blazquez et al., 1998; Moon et al., 2003; Eriksson et al., 2006; Achard et al., 2007), the underlying mechanism is largely elusive. Interestingly, several studies have revealed that DELLA exerts its biological functions through interacting with other transcription factors. For example, DELLA regulates hypocotyl elongation by interacting with PHYTOCHOME INTERACTING FACTORs (PIFs) (de Lucas et al., 2008), contributes to plant defense by interacting with JASMONATE ZIM-DOMAIN (JAZ) (Hou et al., 2010; Yang et al., 2012), and participates in secondary metabolism by interacting with MYC2 (Hong et al., 2012).

Here, we demonstrate the existence of crosstalk between GA and miR156 age pathways. DELLA regulates flowering partially through a direct interaction with miR156-targeted SPL transcription factors. The DELLA–SPL interaction inhibits SPL transcriptional activation of MADS box genes and miR172.

RESULTS

RGA Represses Flowering both in Leaves and at Shoot Apices

Under normal conditions, DELLAs are subjected to GA-induced proteolysis. To reveal the role of GA in flowering, we expressed *RGAd17*, the GA-insensitive form of *RGA* (Dill et al., 2001), from its own upstream regulatory sequence (*ProRGA*:*RGAd17*). *ProRGA*:*RGAd17* phenocopied the GA-deficient mutant, developed small dark green leaves, and delayed flowering (see Supplemental Figure 1 online). Both phloem and SAM have been shown to play critical roles in the floral induction. To understand where RGA regulates flowering, we generated transgenic plants in which *RGAd17* was expressed from either a phloem-specific promoter, *SUC2* (Truernit and Sauer, 1995), or a meristem-specific promoter, *FD* (Abe et al., 2005).

In long-day conditions, the wild-type plants began to flower with ~12 leaves. Both *ProSUC2*:*RGAd17* and *ProFD*:*RGAd17* exhibited a late flowering phenotype, producing more than 20 leaves at the time of bolting (Figures 1A to 1C). In short-day conditions, the flowering of the wild type was greatly delayed, because of the absence of photoperiodic input (Figure 1D). *ProSUC2*:*RGAd17* plants flowered nearly at the same time as the wild type, whereas *ProFD*:*RGAd17* severely blocked the floral transition (Figures 1E and 1F). Six out of 40 T1 *ProFD*:*RGAd17* plants failed to flower. Taken together, these results indicate that RGA regulates flowering via two distinct mechanisms: it suppresses flowering both in the leaves and at the shoot apices in long-day conditions and delays flowering at the shoot apices in short-day conditions.

RGA Represses Flowering through *FT* and miR172 in Leaves under Long-Day Conditions

To assess whether the late flowering phenotype of *ProSUC2*:*RGAd17* in long-day conditions was caused by a low amount of *FT*, we performed quantitative real-time PCR. To facilitate the expression analyses, we chose one representative T3 line of *ProFD*:*RGAd17* and *ProSUC2*:*RGAd17*. Both of these flowered late under long-day or short-day conditions (see Supplemental Figure 2 online).

The leaves of wild-type, *ProFD*:*RGAd17*, and *ProSUC2*:*RGAd17* plants were collected at zeitgeber time 16, when *FT* shows the highest expression level (Kobayashi et al., 1999). Compared with wild-type and *ProFD*:*RGAd17* plants, the transcript level of *FT* was markedly less in *ProSUC2*:*RGAd17* (Figure 2A), indicating that RGA is able to repress *FT* in the vascular tissue of the leaves. In agreement with this finding, it has been shown that GA was able to induce *FT* expression in long-day conditions (Hisamatsu and King, 2008; Porri et al., 2012).

Recent studies have demonstrated that miR172, which is activated by miR156-targeted SPLs, targets *AP2*-like transcription factors that negatively control *FT* expression in leaves (Mathieu et al., 2009; Yant et al., 2010). Overexpression of *SCHLAFMUTZE* (*SMZ*) or *SCHNARCHZAPFEN* (*SNZ*), two miR172-targed AP2-like

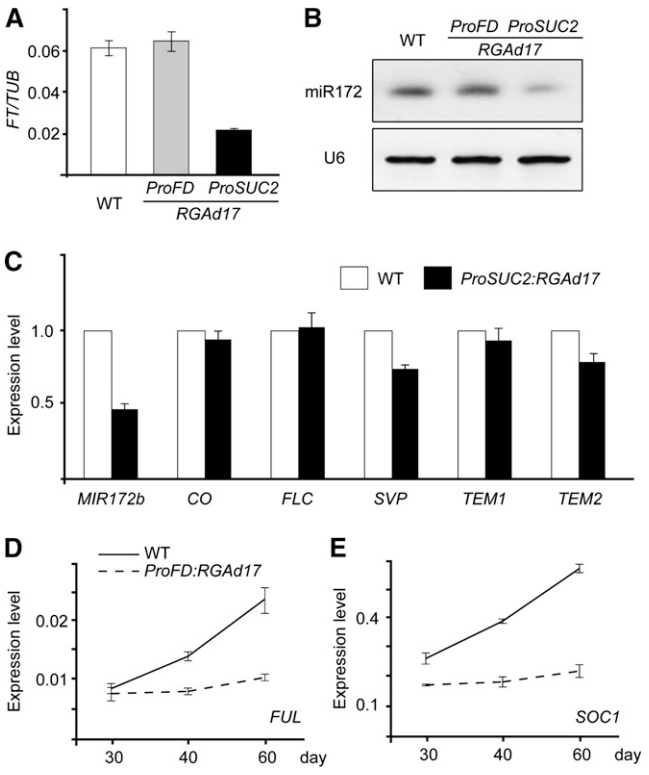

Figure 2. RGA Represses Flowering through *FT* and MADS Box Genes.

(A) Expression of *FT* normalized to β-*TUBULIN-2* (*TUB*) in the wild type (WT) and plants expressing *RGAd17* under the *FD* or *SUC2* promoters.
(B) Expression of miR172 by small RNA gel blot. The amount of U6 was monitored as loading control.
(C) Expression of *MIR172b* and *FT* regulators.
The leaves of wild-type and *ProSUC2*:*RGAd17* plants were used for expression analyses by quantitative real-time–PCR. Plants were grown in long-day conditions for 14 d, and the leaves were harvested at zeitgeber time 16. Expression was normalized to that of β-*TUBULIN-2*. Expression in the wild type was set as 1 for each gene. Two biological replicates were performed with similar results. Error bars represent ±SE (n = 3).
(D) and **(E)** Expression of *FUL* **(D)** and *SOC1* **(E)**. The shoot apices of short-day–grown wild-type and *ProFD*:*RGAd17* plants were harvested at different time points and subjected to quantitative real-time PCR analyses. Error bars represent ±SE (n = 3).

genes, results in a decrease in *FT* expression and a late flowering phenotype in long-day conditions (Mathieu et al., 2009). To test whether DELLA represses *FT* through the SPL-miR172-AP2 module, we analyzed the level of miR172. Compared with wild-type and *ProFD:RGAd17* plants, the level of mature miR172 was much lower in the leaves of *ProSUC2:RGAd17* plants (Figure 2B). Consistent with this, the accumulation of the primary transcript of *MIR172b*, one of the five coding genes of miR172, was accordingly less (Figure 2C).

We then examined the expression of miR172-targeted AP2-like genes, including *AP2*, *SMZ*, *SNZ*, *TARGET OF EAT1* (*TOE1*), *TOE2*, and *TOE3* (Rhoades et al., 2002). The transcript levels of all these genes except those of *SMZ* were not greatly changed (see Supplemental Figure 3 online), which is probably because miR172 controls its targeted genes mainly through the translational inhibition (Aukerman and Sakai, 2003; Chen, 2004; Schwab et al., 2005).

In addition to the miR172-AP2 module, the expression of *FT* is regulated by other transcriptional regulators, such as *CO*, *FLC*, *SVP*, and *TEM* (Searle et al., 2006; Castillejo and Pelaz, 2008; Li et al., 2008). The expression of these genes was not significantly altered in *ProSUC2:RGAd17* in comparison with wild-type and *ProFD:RGAd17* plants (Figure 2C).

To confirm that RGA suppresses flowering through the miR172-AP2-FT module in leaves, we expressed *MIR172a* or *FT* from the *SUC2* promoter in wild-type and *ProSUC2:RGAd17* plants. Both *ProSUC2:FT* and *ProSUC2:MIR172a* flowered earlier than the wild type and were sufficient to suppress the late flowering phenotype of *ProSUC2:RGAd17* under long-day conditions (Figure 3; see Supplemental Figure 4 online).

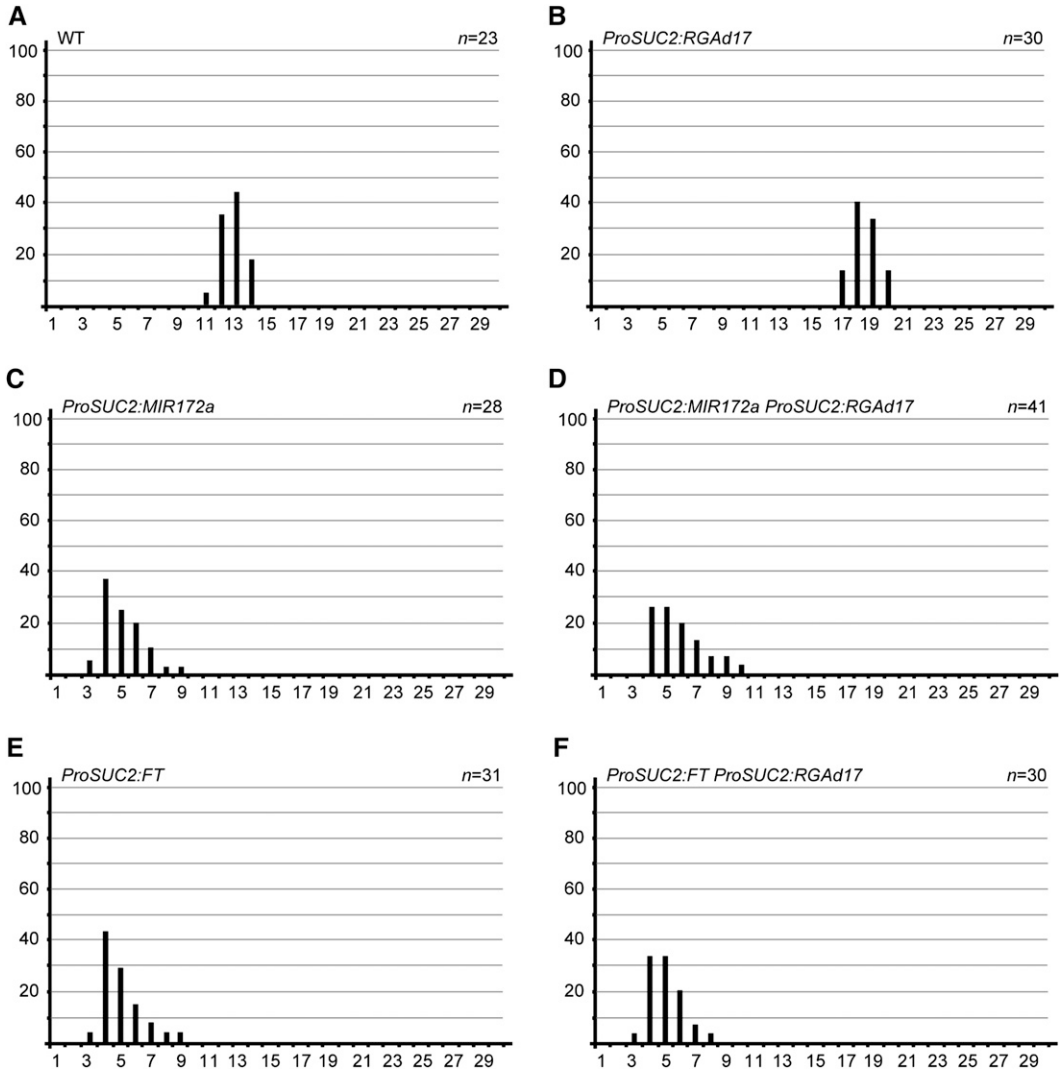

Figure 3. RGA Represses Flowering through miR172-AP2-FT in Leaves.

Flowering time of wild-type (WT), *ProSUC2:RGAd17*, *ProSUC2:MIR172a*, *ProSUC2:FT*, *ProSUC2:RGAd17 ProSUC2:MIR172a*, and *ProSUC2:RGAd17 ProSUC2:FT* plants under long-day conditions. Flowering frequency of T1 transgenic lines is shown as a histogram, with the *y* axis indicating percentage of plants that flower with a given number of leaves. The *x* axis indicates the number of leaves.

RGA Represses Flowering through MADS Box Genes at Shoot Apex

We have shown that *ProFD:RGAd17* delays flowering at the shoot apex under both long-day and short-day conditions (Figure 1). At the shoot apex, the transition from the vegetative to the reproductive phase is executed by the MADS box genes, such as *FUL* and *SOC1*. We extracted the RNAs from the shoot apices of wild-type and *ProFD:RGAd17* plants of different ages in short-day conditions. In 20-d-old seedlings, *FUL* and *SOC1* transcripts accumulated to a similar level in *ProFD:RGAd17* plants as in the wild type (Figures 2D and 2E). As the plants grew, the expression of *FUL* and *SOC1* was gradually increased in the wild type. However, we did not observe the same increase in both genes in *ProFD:RGAd17* plants (Figures 2D and 2E). Under long-day conditions, the expression of *FUL* and *SOC1* was also decreased in *ProFD:RGAd17* in comparison with the wild type (see Supplemental Figure 5 online). These results indicate that RGA blocks the activation of MADS box genes at the shoot apices. Consistent with this, it has been shown that the activation of *SOC1* is attenuated in the *ga1-3* mutant and that overexpression of *SOC1* rescues the flowering phenotype of the *ga1-3* plants in short-day conditions (Moon et al., 2003).

Overexpression of miR156 Reduces the GA Response in Flowering

To understand the genetic interaction between GA and miR156, we studied the GA response of the wild type, the miR156 overexpression line (*Pro35S:MIR156*), in which miR156 was expressed from the *35S* promoter (Schwab et al., 2005), and the miR156 target mimicry line (*Pro35S:MIM156*), which reduces miR156 activity (Franco-Zorrilla et al., 2007; Wang et al., 2008; Todesco et al., 2010). miR156 has been shown to affect leaf initiation rate (Wang et al., 2008); therefore, we measured the flowering time by counting both the number of leaves and the number of days until the plants started to flower.

Under long day conditions, 5-d-old seedlings were sprayed once with 50 μM of gibberellic acid (GA_3). The photoperiod pathway plays a predominant role in long-day conditions; therefore, the flowering response to GA was largely masked (see Supplemental Figure 6 online). We performed the same GA treatment assay under short-day conditions. As shown in Figure 4, application of GA_3 was sufficient to accelerate flowering in the wild-type plants. The number of leaves or days was accordingly decreased by 33 or 19%, respectively (Figures 4A to 4C). By contrast, *Pro35S:MIR156* significantly reduced GA sensitivity. The GA_3-treated *Pro35S:MIR156* plants flowered almost as late as the mock-treated plants (Figures 4A and 4B; see Supplemental Figure 7 online). We only observed 4.4% reduction in the number of days and 3.7% reduction in the number of leaves (Figure 4C).

To understand whether the change in GA response of *Pro35S:MIR156* plants under short-day conditions is caused by a reduction in MADS box genes, we analyzed the expression of *SOC1* and *FUL*. We sprayed 50-d-old short-day–grown plants with 50 μM of GA_3, and their shoot apices were collected after 6 h. The expression of *SOC1* and *FUL* was elevated in the GA_3-treated wild-type plants but not in *Pro35S:MIR156* plants (Figures 4D and 4E).

Expression of *SPL* and *DELLA*

In the *Arabidopsis* genome, miR156-targeted *SPLs* can be divided into two groups, represented by *SPL3* and *SPL9* (Guo et al., 2008; Xing et al., 2010). To determine whether RGA regulates the transcription of *SPL*s, we analyzed the mRNAs of *SPL3* and *SPL9* in wild-type and *Pro35S:RGAd17* plants at different time points in short-day conditions. There was no significant change in *SPL9* transcript levels between wild-type and *Pro35S:RGAd17* plants (Figure 5A). *SPL3* exhibited a distinct expression pattern: its mRNAs gradually increased in wild-type plants but increased less in *Pro35S:RGAd17* plants (Figure 5B). In agreement with this finding, a recent report has shown that *SPL3* level was repressed by paclobutrazol (PAC), a GA biosynthesis inhibitor (Jung et al., 2012). Compared with the wild type, the expression of *DELLAs*, including *RGA*, *RGL1*, and *GAI*, was not greatly altered in either *Pro35S:MIR156* or *Pro35S:MIM156* plants (Figure 5C).

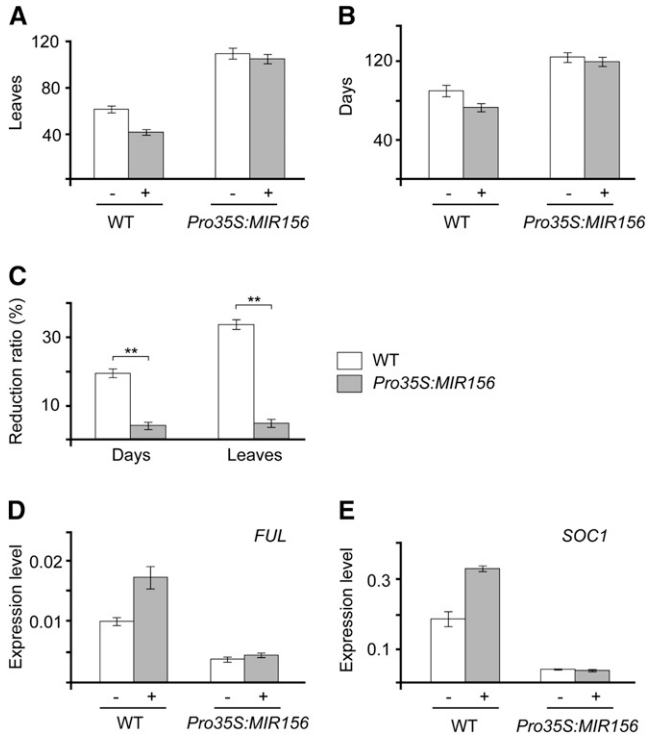

Figure 4. *Pro35S:MIR156* Reduces the GA Response.

(A) and **(B)** GA response of wild-type (WT) and *Pro35S:MIR156* plants under short-day conditions. We sprayed 7-d-old seedlings with 50 μM of GA_3 (+) or ethanol (mock, −). The number of leaves **(A)** and the days to flowering **(B)** were counted.

(C) The reduction ratio in response to GA. The reduction ratio was calculated as (number of leaves/days [mock] − number of leaves/days [GA_3] / number of leaves/days [mock]). **, Student's *t* test, $P < 0.01$.

(D) and **(E)** Expression of *SOC1* and *FUL* in 50-d-old GA_3-treated wild-type and *Pro35S:MIR156* plants in short-day conditions. The shoot apices were collected 6 h after treatment. Error bars represent ±SE ($n = 3$).

Expression of GA Biosynthetic and Catabolic Genes

To understand whether SPL affects GA biosynthesis, we monitored the expression of several GA biosynthetic genes that are highly expressed in leaves, including *GA2-oxidase-1* (*GA2ox-1*), *GA2ox-2*, *GA2ox-6*, *GA3-oxidase-1* (*GA3ox-1*), *GA20-oxidase-1* (*GA20ox-1*), and *GA20ox-2*. GA3ox and GA20ox are responsible for the biosynthesis of bioactive GA_4, whereas GA2ox catalyzes the deactivation of GA_4 by oxidation (Figure 6A) (Eriksson et al., 2006; Yamaguchi, 2008). Compared with the wild type, the expression of the genes encoding *GA2ox-1*, *GA3ox-1*, *GA20ox-1*, and *GA20ox-2* was not changed in either *Pro35S*:*MIR156* or *Pro35S*:*MIM156* plants. The transcript levels of *GA2ox-2* and *GA2ox-6* were moderately decreased in *Pro35S*:*MIM156* and increased in *Pro35S*:*MIR156* plants (Figure 6B). To test whether the change in *GA2ox* expression results in an increase in bioactive GA, we measured the content of GAs, including GA_4, GA_{53}, and GA_{12}. As shown in Figure 6C, *Pro35S*:*MIM156* and *Pro35S*:*MIR156* plants accumulated the same amount of GA_4, one of the bioactive forms of GA, as wild-type plants (Figure 6C).

Genetic Interaction between Age and GA Pathway

To further elucidate the genetic interaction between DELLA and SPL, we overexpressed miR156 in the *della* pentuple mutant (Landsberg *erecta* [L*er*] background) (Feng et al., 2008). The *della* mutant flowered earlier than the wild type (L*er*) under long-day conditions. Overexpression of *MIR156* resulted in a delay of flowering in both the wild type (L*er*) and *della* mutant background (Figures 7A and 7B; see Supplemental Figure 8 online).

SPL9 and SPL15 play a dominant role within miR156-targeted SPLs. The *spl9 spl15* double mutant shows a similar but weak phenotype as the miR156 overexpression line (Schwarz et al., 2008; Wang et al., 2008). Under long-day conditions, *ProSPL9*:*rSPL9* plants, where the miR156-resistant form of *SPL9* (*rSPL9*) was expressed under its own regulatory sequence (Wang et al., 2008), promoted flowering in long-day conditions (Figure 7C). We crossed *ProSPL9*:*rSPL9* to *ProRGA*:*RGAd17*. *ProSPL9*:*rSPL9 ProRGA*:*RGAd17* plants developed the same small dark green leaves as *Pro35S*:*RGAd17* and flowered earlier than *ProRGA*:*RGAd17* (Figure 7C; see Supplemental Figure 9 online). Taken together, our genetic and expression analyses indicate that miR156-targeted SPLs are essential for the floral induction by GAs and that DELLA represses flowering partially through miR156-targeted SPLs.

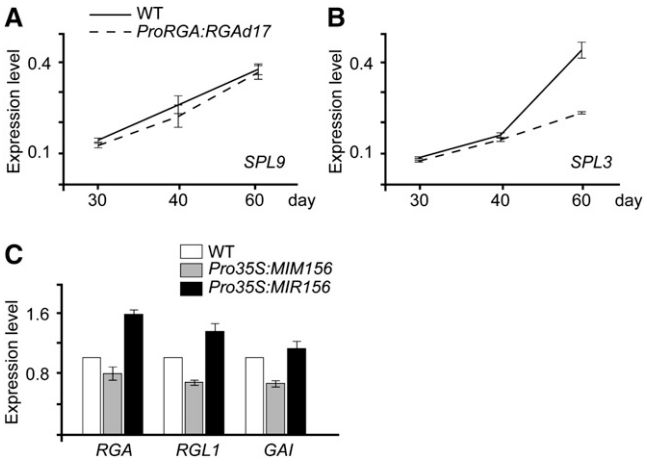

Figure 5. Expression of *SPLs* and *DELLAs*.

(A) and **(B)** Expression of *SPL3* **(A)** and *SPL9* **(B)** in wild-type (WT) and *ProRGA*:*RGAd17* plants. Error bars represent ±SE (n = 3). The shoot apices of short-day–grown plants were harvested at different time points.
(C) Expression of *DELLAs* in wild-type, *Pro35S*:*MIM156*, and *Pro35S*:*MIR156* plants. We used 20-d-old plants grown in short-day conditions for expression analyses. Error bars represent ±SE (n = 3).

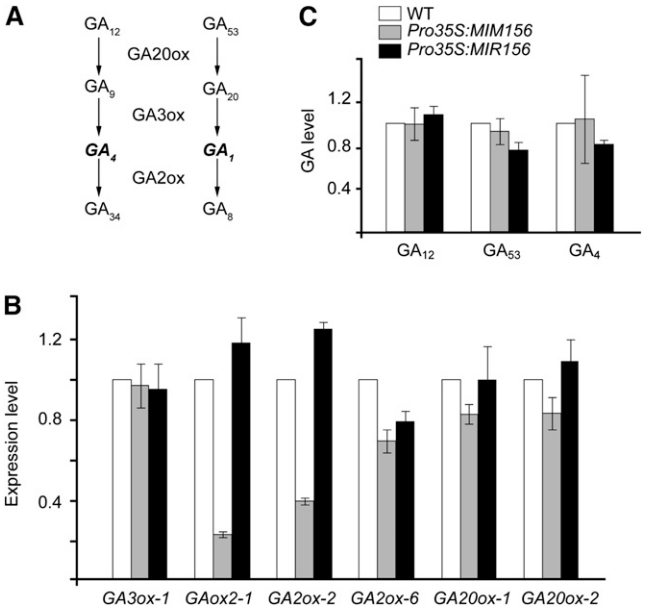

Figure 6. Expression of GA Biosynthetic and Catabolic Genes.

(A) GA biosynthetic and catabolic pathway. The bioactive forms of GA are labeled in bold italic.
(B) Expression of *GA3ox*, *GA20ox*, and *GA2ox* in 15-d-old plants grown in short-day conditions. Error bars represent ±SE (n = 3).
(C) GA measurement. The level in the wild type (WT) was set to 1. Error bars represent ±SE (n = 3).

RGA Binds Directly to SPLs

Because of lack of a canonical DNA binding domain, DELLA regulates plant development and physiology by interacting with other transcription factors, such as PIFs, SCL3, MYC2, and JAZ (de Lucas et al., 2008; Feng et al., 2008; Hou et al., 2010; Zhang et al., 2011; Hong et al., 2012; Yang et al., 2012). Given the fact that both SPLs and RGA regulate the floral transition through the same downstream targets, such as miR172, *FUL*, and *SOC1* (Wang et al., 2009; Wu et al., 2009), we suspected that RGA might directly bind to SPL. To test this hypothesis, we performed yeast two-hybrid assays. A strong interaction was observed when RGA was fused to GAL4 activation domain and SPL9 was fused to GAL4 DNA binding domain (BD) (Figure 8A). This interaction was compromised when the C-terminal domain of SPL9 was deleted

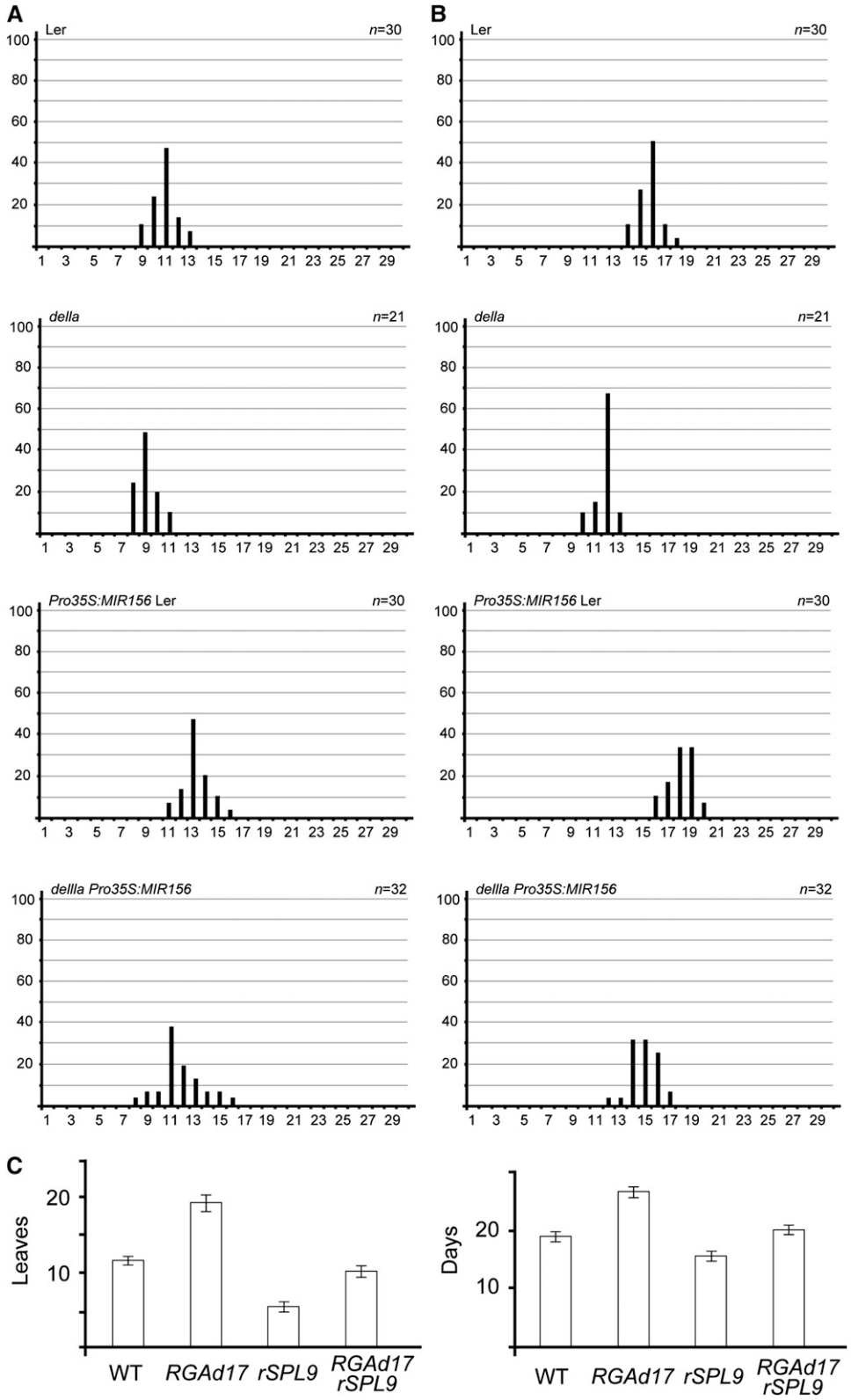

Figure 7. Genetic Interaction between GA and miR156.

(A) and **(B)** Flowering time of *della* and *della Pro35S*:*MIR156* under long-day conditions. The *x* axis indicates the number of leaves **(A)** or the number of days **(B)**. Flowering frequency of *della* homozygous plants and T1 *della Pro35S*:*MIR156* transgenic lines are shown as a histogram, with the *y* axis indicating percentage of plants that flower with a given number of leaves.

(C) Flowering time of wild-type (WT), *ProRGA*::*RGAd17*, *ProSPL9*:*rSPL9*, *and ProRGA*:*RGAd17 ProSPL9*:*rSPL9* plants under long-day conditions. Homozygous *ProRGA*:*RGAd17*, *ProSPL9*:*rSPL9*, and *ProRGA*:*RGAd17 ProSPL9*:*rSPL9* plants were used for flowering time measurements.

(SPL9dC) (Figure 8B). Consistent with this finding, an SPL3 mutant that only harbors the SBP DNA binding domain also failed to interact with RGA (Gandikota et al., 2007) (Figure 8B), suggesting that the C-terminal domain of SPL9 is responsible for its interaction with RGA. Yeast two-hybrid assays further demonstrated the widespread interactions between DELLAs and miR156-targeted SPLs (see Supplemental Figure 10 online).

To examine the interaction between SPL9 and RGA in vivo, we used a bimolecular fluorescence complementation (BiFC) assay in *Nicotiana benthamiana* (Chen et al., 2008). rSPL9 was in-frame fused to the N-terminal half of firefly luciferase (LUC) (rSPL9-LUC^n), and RGA was fused to the C-terminal half of LUC (LUC^c-RGA). Luminescence was detected when the leaves were infiltrated with LUC^c-rSPL9/RGA-LUC^n, but not in those infiltrated with LUC^c-rSPL9/LUC^n or LUC^c/RGA-LUC^n (Figure 8C).

To further confirm the direct interaction between SPL9 and RGA, we performed a coimmunoprecipitation (CoIP) experiment using an *N. benthamiana* transient expression assay. Hemagglutinin (HA)-tagged RGAd17 and green fluorescent protein (GFP)-tagged rSPL9 were transiently expressed in the leaves of *N. benthamiana*. Protein extract of RGAd17-3xHA or RGAd17-3xHA GFP-rSPL9 was immunoprecipitated by the antibody against SPL9. In the immunoprecipitation fraction, RGAd17-3xHA was readily detected in the sample of RGAd17-3xHA GFP-rSPL9 but not in that of RGAd17-3xHA (Figure 8D).

Interaction between DELLA and SPL Interferes with SPL Transcriptional Activity

To understand whether DELLA interferes with SPL transcriptional activity, we examined the expression of *SOC1* and *MIR172b* in *ProSPL9:rSPL9 ProRGA:RGAd17* plants. Consistent with previous reports (Wang et al., 2009; Wu et al., 2009), the expression of *SOC1* and *MIR172b* was upregulated in *ProSPL9:rSPL9* in comparison with the wild type (Figure 9A). If DELLA interferes with the transcriptional activity of SPL, one would expect that the activation of *SOC1* and *MIR172b* by SPL would be compromised by the increased level of RGA. Indeed, the transcripts of *SOC1* and *MIR172b* accumulated to the same level in *ProSPL9:rSPL9 ProRGA:RGAd17* as in the wild type (Figure 9A).

Next, we studied the sensitivity of wild-type, *ProSPL9:rSPL9*, *Pro35S:MIR156* plants to PAC. To verify the treatment efficiency, we examined the expression of *NOD26-LIKE INTRINSIC PROTEIN* (*NOD26*, At4g19030) and *LIPID TRANSFER PROTEIN3* (*LTP3*, At5g59320), both of which are the direct targets of the DELLA-PIF3 module (de Lucas et al., 2008; Feng et al., 2008). After 2 d of the treatment with PAC, the expression of *NOD26* and *LTP3* was greatly decreased (see Supplemental Figure 11 online). We observed a similar reduction in *SOC1* and *MIR172b* transcripts in the PAC-treated wild-type plants, whereas the expression of both genes was insensitive to PAC in *ProSPL9:rSPL9* and *Pro35S:MIR156* plants (Figures 9B and 9C).

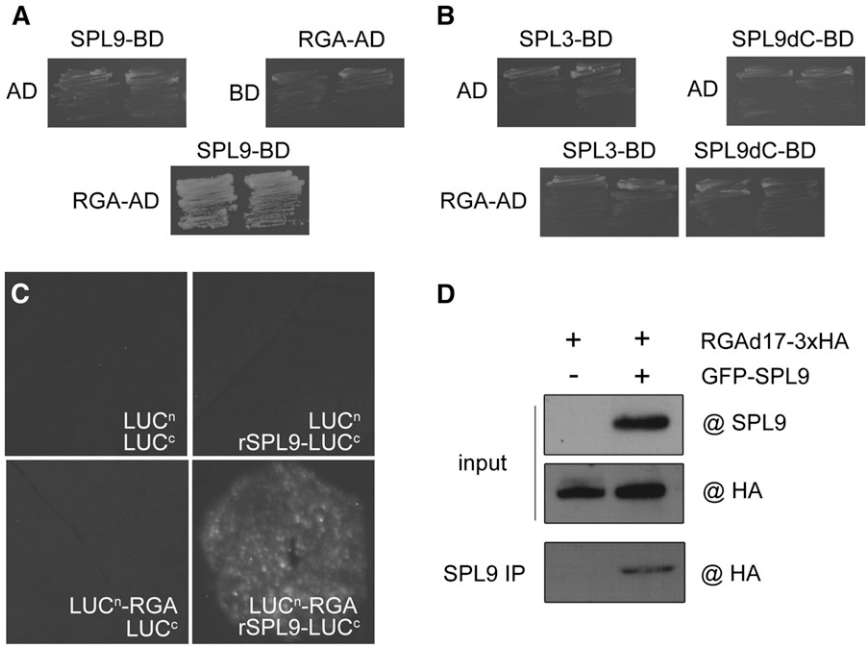

Figure 8. RGA Directly Interacts with SPL9.

(A) Yeast two-hybrid assay. SPL9 was fused to GAL4 BD and RGA to GAL4 activation domain. Interactions were examined on SD/-Leu/-Trp/-His plates supplemented with 15 mM of 3-amino-1,2,4-triazole. Two independent clones are shown.

(B) SPL9 binds to RGA through its C-terminal. SPL3 and SPL9dC were fused to BD.

(C) BiFC analyses. *N. benthamiana* leaves were infiltrated with agrobacteria. The combinations of LUC^c-rSPL9 with LUC^n and LUC^c with RGA-LUC^n were used as negative controls.

(D) CoIP analyses. Soluble protein extract was immunoprecipitated with anti-SPL9 antibody. RGAd17-3xHA proteins were detected by immunoblot with anti-HA antibody.

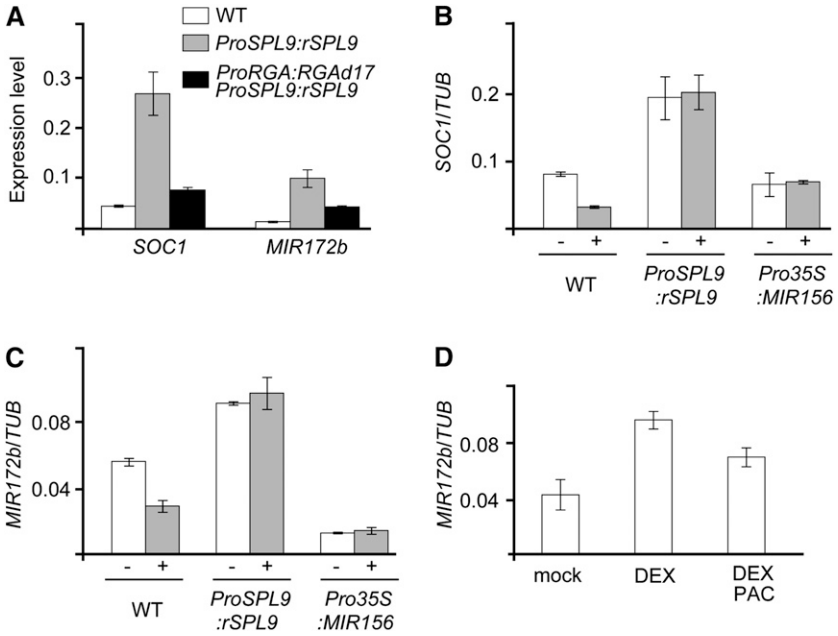

Figure 9. RGA Impairs the Activation of miR172 and *SOC1* through SPL9.

(A) RGA interferes with the activation of *SOC1* and *MIR172b*. We analyzed 30-d-old short-day–grown wild-type (WT), *ProSPL9:rSPL9*, and *ProRGA:RGAd17 ProSPL9:rSPL9* plants. Error bars represent ±SE (n = 3).

(B) and **(C)** Expression of *SOC1* **(B)** and *MIR172b* **(C)** in the PAC-treated wild-type, *ProSPL9:rSPL9*, and *Pro35S:MIR156* plants. We collected 20-d-old short-day–grown seedlings 2 d after treatment. Error bars represent ±SE (n = 3).

(D) Inducible expression of *MIR172b*. We sprayed 10-d-old long-day–grown *ProSPL9:rSPL9-GR* seedlings with DEX, DEX + PAC, or ethanol (mock) for 12 h. Error bars represent ±SE (n = 3).

To further confirm these results, we used an inducible system in which *rSPL9* fused to the rat glucocorticoid receptor (GR) was expressed under its regulatory sequence (*ProSPL9:rSPL9-GR*) (Wang et al., 2009). Treatment with the GR ligand dexamethasone (DEX) resulted in a threefold increase in *MIR172b* transcripts after 12 h (Figure 9D). By contrast, we only observed a 1.5-fold induction in *MIR172b* when 50 μM of PAC was coapplied. Taken together, these observations indicate that a high level of RGA impairs the activation of MADS box genes and miR172 through SPL.

DISCUSSION

Integration of Flowering Time Pathways

Forward and reverse genetics have identified five flowering pathways in *Arabidopsis*, including photoperiod, vernalization, GA, autonomous, and age pathways (Amasino, 2010; Srikanth and Schmid, 2011). Elucidation of how these pathways are integrated is of great importance in understanding how plants flower in response to diverse developmental and environmental signals. Previous results have shown that vernalization and autonomous pathways converge at *FLC*, which encodes a MADS box–type flowering repressor (Simpson, 2004). Interestingly, FLC could also inactivate *FT* in leaves, providing a molecular link between vernalization and photoperiod pathways (Searle et al., 2006).

The age pathway is governed by miR156, the level of which gradually decreases as age increases (Wu and Poethig, 2006; Wang et al., 2009). The integration between photoperiod and age pathway has been extensively studied. In leaves, miR156-SPL acts in parallel with CO, both of which are positive regulators of *FT*. SPL promotes flowering through the miR172-AP2-FT signaling cascade (Mathieu et al., 2009; Wang et al., 2009; Yant et al., 2010). At the shoot apex, the photoperiod pathway acts upstream of SPL. The FT–14-3-3–FD complex activates the expression of *SPL3* and *SPL4* (Jung et al., 2012).

Our results reveal that age and GA pathways are integrated through a direct physical interaction between SPL and DELLA. The binding of DELLA to SPLs attenuates SPL transcriptional activities toward FT and MADS box genes, subsequently blocking the floral transition. It will be interesting to see how the age pathway is integrated into vernalization and autonomous pathways. Indeed, a recent study in *Arabis alpina*, a perennial herb, has revealed that the vernalization response of this perennial plant is age-dependent (Wang et al., 2011). Given the fact that the transcript level of *FLC* is not altered in either *Pro35S:MIM156* or *Pro35S:MIR156 Arabidopsis* plants (Wang et al., 2009), it is unlikely that the age pathway regulates vernalization through modulating *FLC* expression.

DELLA Represses Flowering via Distinct Mechanisms

Our results demonstrate that DELLA regulates flowering via two distinct mechanisms (see Supplemental Figure 12 online). Under short-day conditions, miR156-targeted SPLs play a major role in

flowering by activating MADS box genes at the shoot apex. DELLAs delay the floral transition through interfering with the transcriptional activities of SPL. Under long-day conditions, in addition to a similar role at the shoot apex, the interaction between DELLA and SPL leads to a decrease of miR172. As a result, the increased level of AP2-like transcription factors represses flowering through inactivating *FT*.

Pro35S:MIR156 still responds to GA; therefore, additional flowering targets of DELLA must exist. Indeed, a recent report has shown that simultaneous inactivation of two GA-responsive GATA transcription factors, GATA, NITRATE-INDUCIBLE, CARBON-METABOLISM INVOLVED (GNC) and GNC-LIKE/CYTOKININ-RESPONSIVE GATA FACTOR1 (GNL), partially rescues the flowering defect of *ga1-3* plants in short-day conditions (Richter et al., 2010). Another potential flowering target of DELLA is *SVP*, which encodes a MADS box–type floral repressor. The expression of *SVP* is reduced in the GA-treated plants and increased in a GA-deficient mutant (Li et al., 2008). Moreover, because the level of *SPL3* was decreased in the shoot apices of *ProFD:RGAd17* plants, we could not exclude the possibility that DELLA controls flowering through modulating the expression of *SPLs*. Indeed, a recent study has suggested that GA could promote flowering through SPL3 (Porri et al., 2012).

DELLA and SPL in Vegetative Phase Transition

In addition to a role in flowering, GA is essential for the expression of adult phase traits (Chien and Sussex, 1996; Poethig, 2003). In *Arabidopsis*, juvenile leaves only develop trichomes on their adaxial (upper) sides, whereas adult leaves produce trichomes on their adaxial and abaxial (lower) sides. The GA-deficient mutant delays the appearance of abaxial trichomes, whereas exogenous application of GA accelerates the formation of abaxial trichomes (Telfer et al., 1997).

miR156-targeted SPLs exert a similar role as that of GA in vegetative phase transition. The SPL level is correlated with abaxial trichome production (Wu and Poethig, 2006; Wu et al., 2009). DELLA directly binds to SPL; therefore, it is plausible that GA could promote abaxial trichome formation through releasing the inhibition of DELLA on SPL. However, a recent study has shown that application of GA_3 induces abaxial trichome formation in the miR156 overexpression line, suggesting that GA is able to promote abaxial trichome formation independent of SPL (Schwarz et al., 2008). Whether GA regulates the display of adult vegetative phase traits through SPL awaits further investigation.

METHODS

Plant Materials

Arabidopsis thaliana plants, ecotypes Columbia and L*er*, and *Nicotiana benthamiana* were grown at 21°C in long days (16-h light/8-h dark) or short days (8-h light/16-h dark). *Pro35S:MIR156*, *Pro35S:MIM156*, *ProSPL9:rSPL9*, and *ProSPL9:rSPL9-GR* have been described elsewhere (Wang et al., 2008; Wang et al., 2009). The *della* mutant (N16298) was ordered from the Nottingham Arabidopsis Stock Centre (www.*Arabidopsis*.info). For GA and PAC treatment, 50 μM of GA_3 (Sigma-Aldrich) and 50 μM of PAC were used. For DEX induction experiment, 10 μM of DEX or 10 μM of DEX plus 50 μM of PAC was used.

Constructs and Plant Transformation

For RGAd17 constructs, *RGAd17* was cloned into the binary constructs behind the *RGA*, *SUC2*, or *FD* promoter (Wang et al., 2008). For *FT* and *MIR172a* constructs, the coding region of *FT* and a 410-bp fragment harboring the stem loop of *MIR172a* was PCR amplified and cloned into the binary construct behind the *pSUC2* promoter. For yeast two-hybrid constructs, the cDNAs of *SPL2*, *SPL3*, *SPL9*, *SPL9dC*, *SPL10*, and *SPL11* were PCR amplified and cloned into pGBKT7 or pGADT7 (Clontech). *RGA* was cloned into pGADT7. The pGBKT7 series of *GAI*, *RGA*, *RGL1*, *RGL2*, and *RGL3* constructs was generated as described in de Lucas et al. (2008). BiFC constructs were generated as described elsewhere (Chen et al., 2008; Gou et al., 2011). For CoIP constructs, *RGAd17* and *rSPL9* was PCR amplified and cloned into the binary constructs with 3xHA or GFP tag. The oligonucleotide primers for these constructs are given in Supplemental Table 1 online. The constructs were delivered into *Agrobacterium tumefaciens* strain GV3101 (pMP90) by the freeze-thaw method. Transgenic plants were generated by the floral dipping method (Clough and Bent, 1998) and were screened with 0.05% glufosinate (Basta) on soil or 50 μg/mL of hygromycin on one-half–strength Murashige and Skoog plate.

Flowering Time Measurement and Expression Analyses

Flowering time was measured by counting the total number of leaves (rosette and cauline leaves) and the number of days to flower (when the floral buds are visible).

Total RNA was extracted with TRIzol reagent (Invitrogen). A total of 1 μg of total RNA was DNase I–treated and used for cDNA synthesis with oligo (dT) primer and RevertAid reverse transcriptase (Fermentas). Quantitative real-time–PCR was performed with SYBR-Green PCR Mastermix (TaKaRa), and amplification was real-time monitored on Mastercycler Realplex^2 (Eppendorf). Quantitative real-time PCR primers for *FT*, *MIR172b*, *SOC1*, *FUL*, *SPL3*, *SPL9*, and *TUB* have been described elsewhere (Wang et al., 2009; Wu et al., 2009). Other oligonucleotide primers are given in Supplemental Table 1 online.

Yeast Two-Hybrid Assay

Plasmids were transformed into yeast strain AH109 (Clontech) by the lithium chloride–polyethyleneglycol method according to the manufacturer's manual (Clontech). The transformants were selected on SD/-Leu/-Trp plates. The interactions were tested on SD/-Leu/-Trp/-His plate with 3-amino-1,2,4,-triazole (Figures 8A and 8B) or SD/-Ade/-Leu/-Trp/-His plate (see Supplemental Figure 10B online). At least 10 individual clones were analyzed.

BiFC Analysis

BiFC assays were performed as described in Gou et al. (2011). *A. tumefaciens* was resuspended in infiltration buffer at OD_{600} = 0.8. *Pro35S:P19-HA* (Papp et al., 2003) was coinfiltrated to inhibit gene silencing. A total of 1 mM of luciferin was infiltrated before LUC activity was monitored after 3 d.

CoIP Analysis

SPL9 antibody was raised against the peptide QHQYLNPPWVFKDNC, corresponding to the residues 299 to 312 of SPL9 (Willget Biotech). Agrobacteria-infiltrated *N. benthamiana* leaves were used for CoIP analyses. The soluble proteins were extracted in the extraction buffer (100 mM of Tris-HCl, 5 mM of EDTA, 100 mM of NaCl, 0.2% Nonidet P-40, 1.0% Triton X-100, pH 7.5). Immunoprecipitation was performed with anti-SPL9 antibody. RGAd17-3xHA fusion proteins were detected by immunoblot with anti-HA-horseradish peroxidase antibody (Roche).

GA Measurement

We harvested 2.0-g 40-d-old short-day–grown plants. Extraction and measurement of GA was performed according to a published protocol (Qi et al., 2011).

Accession Numbers

Sequence data from this article can be found in the Arabidopsis Genome Initiative or GenBank/EMBL databases under the following accession numbers: AP2 (At4g36920); CO (At5g15840); FLC (At5g10140); FUL (At5g60910); FT (At1g65480); GAI (At1g14920); GA20ox-1 (At4g25420); GA20ox-2 (At5g51810); GA2ox-1 (At1g78440); GA2ox-2 (At1g30040); GA2ox-6 (At1g02400); GA3ox-1 (At1g15550); MIR172a (At2g28056); MIR172b (At5g04275); RGA (At2g01570); RGL1 (At1g66350); RGL2 (At3g03450); RGL3 (At5g17490); SOC1 (At2g45660); SPL2 (At5g43270); SPL3 (At2g33810); SPL9 (At2g42200); SPL10 (At1g27370); SPL11 (At1g27360); TEM1 (At1g25560); TEM2 (At1g68840); TOE1 (At2g28550); TOE2 (At5g60120); TOE3 (At5g67180); TUB (At5g62690); SMZ (At2g39250); SNZ (At3g54990); SVP (At2g22540).

Supplemental Data

The following materials are available in the online version of this article.

Supplemental Figure 1. Phenotype of *ProRGA*:*RGAd17* Plants under Long-Day Conditions.

Supplemental Figure 2. Flowering Time of the Wild Type, *ProSUC2*:*RGAd17*, and *ProFD*:*RGAd17*.

Supplemental Figure 3. Expression of miR172 Targets.

Supplemental Figure 4. Flowering Time of ProSUC2:MIR172a ProSUC2:RGAd17 and ProSUC2:FT ProSUC2:RGAd17.

Supplemental Figure 5. Expression of *SOC1* and *FUL* at the Shoot Apex in Long-Day Conditions.

Supplemental Figure 6. GA Response in Long-Day Conditions.

Supplemental Figure 7. GA Response of the Wild Type and *Pro35S*:*MIR156* in Short-Day Conditions.

Supplemental Figure 8. Phenotype of *della Pro35S*:*MIR156* Double Mutant.

Supplemental Figure 9. Phenotype of *ProRGA*::*RGAd17 ProSPL9*::*rSPL9* Double Mutant.

Supplemental Figure 10. Interaction between DELLAs and SPLs in Yeast.

Supplemental Figure 11. Expression of *NOD26* and *LTP3* in Response to PAC.

Supplemental Figure 12. A Model for Integration of GA and miR156 Pathway.

Supplemental Table 1. Oligonucleotide Primer Sequences.

ACKNOWLEDGMENTS

We thank Xiao-Ya Chen and Detlef Weigel for their generous scientific support. This article was supported by the National Natural Science Foundation of China (31222029), Recruitment Program of Global Expects (China), and initiation grants from the National Key Laboratory of Plant Genetics, Shanghai Institute of Plant Physiology, and Shanghai Institutes for Biological Sciences to J.-W.W. and by grants from National Nature Science Foundation (91017013 and 31070327) to Q.-Y.F. Work in the Schmid lab on the regulation on flowering time is supported by the Max Planck Institute for Developmental Biology and by grants from the Deutsche Forschungsgemeinschaft.

AUTHOR CONTRIBUTIONS

J.-W.W. and M.S. designed the research. S.Y., V.C.G., Y.-C.Z., D.H., T.-Q.Z., Y.-H.H., and J.-W.W. performed the experiments. Y.-Q.F., M.S., and J.-W.W. analyzed the data. S.W. and J.-W.W. wrote the article.

Received May 29, 2012; revised August 1, 2012; accepted August 6, 2012; published August 31, 2012.

REFERENCES

Abe, M., Kobayashi, Y., Yamamoto, S., Daimon, Y., Yamaguchi, A., Ikeda, Y., Ichinoki, H., Notaguchi, M., Goto, K., and Araki, T. (2005). FD, a bZIP protein mediating signals from the floral pathway integrator FT at the shoot apex. Science **309:** 1052–1056.

Achard, P., Baghour, M., Chapple, A., Hedden, P., Van Der Straeten, D., Genschik, P., Moritz, T., and Harberd, N.P. (2007). The plant stress hormone ethylene controls floral transition via DELLA-dependent regulation of floral meristem-identity genes. Proc. Natl. Acad. Sci. USA **104:** 6484–6489.

Amasino, R. (2010). Seasonal and developmental timing of flowering. Plant J. **61:** 1001–1013.

An, H., Roussot, C., Suárez-López, P., Corbesier, L., Vincent, C., Piñeiro, M., Hepworth, S., Mouradov, A., Justin, S., Turnbull, C., and Coupland, G. (2004). CONSTANS acts in the phloem to regulate a systemic signal that induces photoperiodic flowering of *Arabidopsis*. Development **131:** 3615–3626.

Aukerman, M.J., and Sakai, H. (2003). Regulation of flowering time and floral organ identity by a MicroRNA and its APETALA2-like target genes. Plant Cell **15:** 2730–2741.

Blazquez, M.A., Green, R., Nilsson, O., Sussman, M.R., and Weigel, D. (1998). Gibberellins promote flowering of *Arabidopsis* by activating the LEAFY promoter. Plant Cell **10:** 791–800.

Cardon, G., Höhmann, S., Klein, J., Nettesheim, K., Saedler, H., and Huijser, P. (1999). Molecular characterisation of the *Arabidopsis* SBP-box genes. Gene **237:** 91–104.

Castillejo, C., and Pelaz, S. (2008). The balance between CONSTANS and TEMPRANILLO activities determines FT expression to trigger flowering. Curr. Biol. **18:** 1338–1343.

Chen, H., Zou, Y., Shang, Y., Lin, H., Wang, Y., Cai, R., Tang, X., and Zhou, J.M. (2008). Firefly luciferase complementation imaging assay for protein-protein interactions in plants. Plant Physiol. **146:** 368–376.

Chen, X. (2004). A microRNA as a translational repressor of APETALA2 in *Arabidopsis* flower development. Science **303:** 2022–2025.

Chien, J.C., and Sussex, I.M. (1996). Differential regulation of trichome formation on the adaxial and abaxial leaf surfaces by gibberellins and photoperiod in Arabidopsis thaliana (L.) Heynh. Plant Physiol. **111:** 1321–1328.

Clough, S.J., and Bent, A.F. (1998). Floral dip: A simplified method for *Agrobacterium*-mediated transformation of *Arabidopsis thaliana*. Plant J. **16:** 735–743.

Corbesier, L., Vincent, C., Jang, S., Fornara, F., Fan, Q., Searle, I., Giakountis, A., Farrona, S., Gissot, L., Turnbull, C., and Coupland, G. (2007). FT protein movement contributes to long-distance signaling in floral induction of *Arabidopsis*. Science **316:** 1030–1033.

de Lucas, M., Davière, J.M., Rodríguez-Falcón, M., Pontin, M., Iglesias-Pedraz, J.M., Lorrain, S., Fankhauser, C., Blázquez, M.A., Titarenko, E., and Prat, S. (2008). A molecular framework for light and gibberellin control of cell elongation. Nature **451:** 480–484.

Dill, A., Jung, H.S., and Sun, T.P. (2001). The DELLA motif is essential for gibberellin-induced degradation of RGA. Proc. Natl. Acad. Sci. USA **98:** 14162–14167.

Eriksson, S., Böhlenius, H., Moritz, T., and Nilsson, O. (2006). GA4 is the active gibberellin in the regulation of LEAFY transcription and *Arabidopsis* floral initiation. Plant Cell **18:** 2172–2181.

Feng, S., et al. (2008). Coordinated regulation of *Arabidopsis thaliana* development by light and gibberellins. Nature **451:** 475–479.

Franco-Zorrilla, J.M., Valli, A., Todesco, M., Mateos, I., Puga, M.I., Rubio-Somoza, I., Leyva, A., Weigel, D., García, J.A., and Paz-Ares, J. (2007). Target mimicry provides a new mechanism for regulation of microRNA activity. Nat. Genet. **39:** 1033–1037.

Gandikota, M., Birkenbihl, R.P., Höhmann, S., Cardon, G.H., Saedler, H., and Huijser, P. (2007). The miRNA156/157 recognition element in the 3′ UTR of the *Arabidopsis* SBP box gene SPL3 prevents early flowering by translational inhibition in seedlings. Plant J. **49:** 683–693.

Gou, J.Y., Felippes, F.F., Liu, C.J., Weigel, D., and Wang, J.W. (2011). Negative regulation of anthocyanin biosynthesis in *Arabidopsis* by a miR156-targeted SPL transcription factor. Plant Cell **23:** 1512–1522.

Griffiths, J., Murase, K., Rieu, I., Zentella, R., Zhang, Z.L., Powers, S.J., Gong, F., Phillips, A.L., Hedden, P., Sun, T.P., and Thomas, S.G. (2006). Genetic characterization and functional analysis of the GID1 gibberellin receptors in *Arabidopsis*. Plant Cell **18:** 3399–3414.

Guo, A.Y., Zhu, Q.H., Gu, X., Ge, S., Yang, J., and Luo, J. (2008). Genome-wide identification and evolutionary analysis of the plant specific SBP-box transcription factor family. Gene **418:** 1–8.

Harberd, N.P. (2003). Botany. Relieving DELLA restraint. Science **299:** 1853–1854.

Hisamatsu, T., and King, R.W. (2008). The nature of floral signals in *Arabidopsis*. II. Roles for FLOWERING LOCUS T (FT) and gibberellin. J. Exp. Bot. **59:** 3821–3829.

Hong, G.J., Xue, X.Y., Mao, Y.B., Wang, L.J., and Chen, X.Y. (2012). *Arabidopsis* MYC2 interacts with DELLA proteins in regulating sesquiterpene synthase gene expression. Plant Cell **24:** 2635–2648.

Hou, X., Lee, L.Y., Xia, K., Yan, Y., and Yu, H. (2010). DELLAs modulate jasmonate signaling via competitive binding to JAZs. Dev. Cell **19:** 884–894.

Huijser, P., and Schmid, M. (2011). The control of developmental phase transitions in plants. Development **138:** 4117–4129.

Jaeger, K.E., and Wigge, P.A. (2007). FT protein acts as a long-range signal in *Arabidopsis*. Curr. Biol. **17:** 1050–1054.

Jung, J.H., Ju, Y., Seo, P.J., Lee, J.H., and Park, C.M. (2012). The SOC1-SPL module integrates photoperiod and gibberellic acid signals to control flowering time in *Arabidopsis*. Plant J. **69:** 577–588.

Kobayashi, Y., Kaya, H., Goto, K., Iwabuchi, M., and Araki, T. (1999). A pair of related genes with antagonistic roles in mediating flowering signals. Science **286:** 1960–1962.

Kobayashi, Y., and Weigel, D. (2007). Move on up, it's time for change—mobile signals controlling photoperiod-dependent flowering. Genes Dev. **21:** 2371–2384.

Lee, J., and Lee, I. (2010). Regulation and function of SOC1, a flowering pathway integrator. J. Exp. Bot. **61:** 2247–2254.

Li, D., Liu, C., Shen, L., Wu, Y., Chen, H., Robertson, M., Helliwell, C.A., Ito, T., Meyerowitz, E., and Yu, H. (2008). A repressor complex governs the integration of flowering signals in *Arabidopsis*. Dev. Cell **15:** 110–120.

Lin, M.K., Belanger, H., Lee, Y.J., Varkonyi-Gasic, E., Taoka, K., Miura, E., Xoconostle-Cázares, B., Gendler, K., Jorgensen, R.A., Phinney, B., Lough, T.J., and Lucas, W.J. (2007). FLOWERING LOCUS T protein may act as the long-distance florigenic signal in the cucurbits. Plant Cell **19:** 1488–1506.

Mathieu, J., Warthmann, N., Küttner, F., and Schmid, M. (2007). Export of FT protein from phloem companion cells is sufficient for floral induction in *Arabidopsis*. Curr. Biol. **17:** 1055–1060.

Mathieu, J., Yant, L.J., Mürdter, F., Küttner, F., and Schmid, M. (2009). Repression of flowering by the miR172 target SMZ. PLoS Biol. **7:** e1000148.

Moon, J., Suh, S.S., Lee, H., Choi, K.R., Hong, C.B., Paek, N.C., Kim, S.G., and Lee, I. (2003). The SOC1 MADS-box gene integrates vernalization and gibberellin signals for flowering in *Arabidopsis*. Plant J. **35:** 613–623.

Murase, K., Hirano, Y., Sun, T.P., and Hakoshima, T. (2008). Gibberellin-induced DELLA recognition by the gibberellin receptor GID1. Nature **456:** 459–463.

Mutasa-Göttgens, E., and Hedden, P. (2009). Gibberellin as a factor in floral regulatory networks. J. Exp. Bot. **60:** 1979–1989.

Papp, I., Mette, M.F., Aufsatz, W., Daxinger, L., Ray, A., van der Winden, J., Matzke, M., and Matzke, A.J. (2003). Evidence for nuclear processing of plant micro RNA and short interfering RNA precursors. Plant Physiol. **132:** 1382–1390.

Peng, J., Carol, P., Richards, D.E., King, K.E., Cowling, R.J., Murphy, G.P., and Harberd, N.P. (1997). The *Arabidopsis* GAI gene defines a signaling pathway that negatively regulates gibberellin responses. Genes Dev. **11:** 3194–3205.

Poethig, R.S. (2003). Phase change and the regulation of developmental timing in plants. Science **301:** 334–336.

Porri, A., Torti, S., Romera-Branchat, M., and Coupland, G. (2012). Spatially distinct regulatory roles for gibberellins in the promotion of flowering of *Arabidopsis* under long photoperiods. Development **139:** 2198–2209.

Qi, W., Sun, F., Wang, Q., Chen, M., Huang, Y., Feng, Y.Q., Luo, X., and Yang, J. (2011). Rice ethylene-response AP2/ERF factor OsEATB restricts internode elongation by down-regulating a gibberellin biosynthetic gene. Plant Physiol. **157:** 216–228.

Rhoades, M.W., Reinhart, B.J., Lim, L.P., Burge, C.B., Bartel, B., and Bartel, D.P. (2002). Prediction of plant microRNA targets. Cell **110:** 513–520.

Richter, R., Behringer, C., Müller, I.K., and Schwechheimer, C. (2010). The GATA-type transcription factors GNC and GNL/CGA1 repress gibberellin signaling downstream from DELLA proteins and PHYTOCHROME-INTERACTING FACTORS. Genes Dev. **24:** 2093–2104.

Samach, A., Onouchi, H., Gold, S.E., Ditta, G.S., Schwarz-Sommer, Z., Yanofsky, M.F., and Coupland, G. (2000). Distinct roles of CONSTANS target genes in reproductive development of *Arabidopsis*. Science **288:** 1613–1616.

Schmid, M., Uhlenhaut, N.H., Godard, F., Demar, M., Bressan, R., Weigel, D., and Lohmann, J.U. (2003). Dissection of floral induction pathways using global expression analysis. Development **130:** 6001–6012.

Schwab, R., Palatnik, J.F., Riester, M., Schommer, C., Schmid, M., and Weigel, D. (2005). Specific effects of microRNAs on the plant transcriptome. Dev. Cell **8:** 517–527.

Schwarz, S., Grande, A.V., Bujdoso, N., Saedler, H., and Huijser, P. (2008). The microRNA regulated SBP-box genes SPL9 and SPL15 control shoot maturation in *Arabidopsis*. Plant Mol. Biol. **67:** 183–195.

Schwechheimer, C., and Willige, B.C. (2009). Shedding light on gibberellic acid signalling. Curr. Opin. Plant Biol. **12:** 57–62.

Searle, I., He, Y., Turck, F., Vincent, C., Fornara, F., Kröber, S., Amasino, R.A., and Coupland, G. (2006). The transcription factor FLC confers a flowering response to vernalization by repressing meristem competence and systemic signaling in *Arabidopsis*. Genes Dev. **20:** 898–912.

Simpson, G.G. (2004). The autonomous pathway: Epigenetic and post-transcriptional gene regulation in the control of *Arabidopsis* flowering time. Curr. Opin. Plant Biol. **7:** 570–574.

Srikanth, A., and Schmid, M. (2011). Regulation of flowering time: All roads lead to Rome. Cell. Mol. Life Sci. **68:** 2013–2037.

Taoka, K., et al. (2011). 14-3-3 proteins act as intracellular receptors for rice Hd3a florigen. Nature **476:** 332–335.

Telfer, A., Bollman, K.M., and Poethig, R.S. (1997). Phase change and the regulation of trichome distribution in *Arabidopsis thaliana*. Development **124:** 645–654.

Todesco, M., Rubio-Somoza, I., Paz-Ares, J., and Weigel, D. (2010). A collection of target mimics for comprehensive analysis of microRNA function in *Arabidopsis thaliana*. PLoS Genet. **6:** e1001031.

Torti, S., Fornara, F., Vincent, C., Andrés, F., Nordström, K., Göbel, U., Knoll, D., Schoof, H., and Coupland, G. (2012). Analysis of the *Arabidopsis* shoot meristem transcriptome during floral transition identifies distinct regulatory patterns and a leucine-rich repeat protein that promotes flowering. Plant Cell **24:** 444–462.

Truernit, E., and Sauer, N. (1995). The promoter of the *Arabidopsis thaliana* SUC2 sucrose-H+ symporter gene directs expression of beta-glucuronidase to the phloem: Evidence for phloem loading and unloading by SUC2. Planta **196:** 564–570.

Wang, J.W., Czech, B., and Weigel, D. (2009). miR156-regulated SPL transcription factors define an endogenous flowering pathway in *Arabidopsis thaliana*. Cell **138:** 738–749.

Wang, J.W., Schwab, R., Czech, B., Mica, E., and Weigel, D. (2008). Dual effects of miR156-targeted SPL genes and CYP78A5/KLUH on plastochron length and organ size in *Arabidopsis thaliana*. Plant Cell **20:** 1231–1243.

Wang, R., Albani, M.C., Vincent, C., Bergonzi, S., Luan, M., Bai, Y., Kiefer, C., Castillo, R., and Coupland, G. (2011). Aa TFL1 confers an age-dependent response to vernalization in perennial *Arabis alpina*. Plant Cell **23:** 1307–1321.

Wigge, P.A., Kim, M.C., Jaeger, K.E., Busch, W., Schmid, M., Lohmann, J.U., and Weigel, D. (2005). Integration of spatial and temporal information during floral induction in *Arabidopsis*. Science **309:** 1056–1059.

Wilson, R.N., Heckman, J.W., and Somerville, C.R. (1992). Gibberellin is required for flowering in Arabidopsis thaliana under short days. Plant Physiol. **100:** 403–408.

Wu, G., Park, M.Y., Conway, S.R., Wang, J.W., Weigel, D., and Poethig, R.S. (2009). The sequential action of miR156 and miR172 regulates developmental timing in *Arabidopsis*. Cell **138:** 750–759.

Wu, G., and Poethig, R.S. (2006). Temporal regulation of shoot development in *Arabidopsis thaliana* by miR156 and its target SPL3. Development **133:** 3539–3547.

Xing, S., Salinas, M., Höhmann, S., Berndtgen, R., and Huijser, P. (2010). miR156-targeted and nontargeted SBP-box transcription factors act in concert to secure male fertility in *Arabidopsis*. Plant Cell **22:** 3935–3950.

Yamaguchi, A., Wu, M.F., Yang, L., Wu, G., Poethig, R.S., and Wagner, D. (2009). The microRNA-regulated SBP-Box transcription factor SPL3 is a direct upstream activator of LEAFY, FRUITFULL, and APETALA1. Dev. Cell **17:** 268–278.

Yamaguchi, S. (2008). Gibberellin metabolism and its regulation. Annu. Rev. Plant Biol. **59:** 225–251.

Yang, D.L., et al. (2012). Plant hormone jasmonate prioritizes defense over growth by interfering with gibberellin signaling cascade. Proc. Natl. Acad. Sci. USA **109:** E1192–E1200.

Yant, L., Mathieu, J., Dinh, T.T., Ott, F., Lanz, C., Wollmann, H., Chen, X., and Schmid, M. (2010). Orchestration of the floral transition and floral development in *Arabidopsis* by the bifunctional transcription factor APETALA2. Plant Cell **22:** 2156–2170.

Zhang, Z.L., Ogawa, M., Fleet, C.M., Zentella, R., Hu, J., Heo, J.O., Lim, J., Kamiya, Y., Yamaguchi, S., and Sun, T.P. (2011). Scarecrow-like 3 promotes gibberellin signaling by antagonizing master growth repressor DELLA in *Arabidopsis*. Proc. Natl. Acad. Sci. USA **108:** 2160–2165.